JACS Au
AN OPEN ACCESS JOURNAL OF THE AMERICAN CHEMICAL SOCIETY

pubs.acs.org/jacsau
Article

Amino Acid Decorated Phenanthroline Diimide as Sustainable Hydrophilic Am(III) Masking Agent with High Acid Resistance

Bin Li,[⊥] Ludi Wang,[⊥] Yu Kang, Hong Cao, Yaoyang Liu, Qiange He, Zhongfeng Li, Xiaoyan Tang, Jing Chen, Li Wang,* and Chao Xu*

Cite This: *JACS Au* 2024, 4, 3668−3678
Read Online

ACCESS | Metrics & More | Article Recommendations | Supporting Information

ABSTRACT: Hydrophilic actinide masking agents are believed to be efficient alternatives to circumvent the extensive hazardous organic solvents/diluents typically employed in the liquid−liquid extraction for nuclear waste management. However, the practical application of hydrophilic ligands faces significant challenges in both synthetic/purification procedures and, more importantly, the acid resistance of the ligands themselves. Herein, we have demonstrated the combination of phenanthroline diimide framework with a biomotif of histidine flanking parts could achieve efficient separation of trivalent lanthanides/actinides (also actinides/actinides) under high acidity of over 1 M HNO_3. This approach leverages the soft−hard coordination properties of *N, O*-hybrid ligands, as well as the energetically favored imides for metal coordination and the multiple protonation of histidine. These factors collectively contribute to the synthesis of an easily accessible, highly water-soluble, superior selective, and acid-resistant Am(III) masking agent. Thus, we have shown in this paper, by proper combination of synthetic *N, O*-hybrid ligand with amino acid, trivalent lanthanide and actinide separation could be efficiently fulfilled in a more sustainable manner.

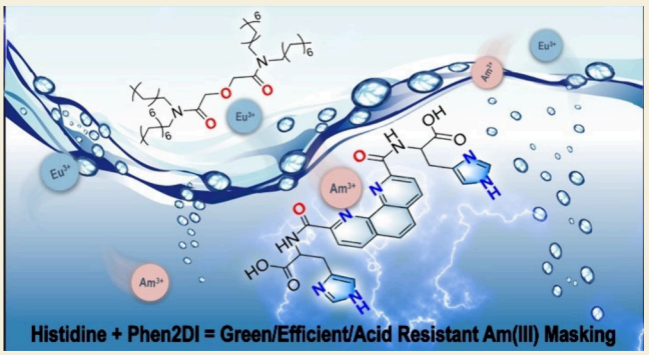

KEYWORDS: *liquid−liquid extraction, lanthanides and actinides separation, acid-resistance, hydrophilic ligands, amino acids*

INTRODUCTION

Nuclear power is believed to be an important zero-emission green energy source with great potential for sustainable solution to the current environmental protection and energy saving.[1,2] However, the proper handling of the associated waste has long been problematic because of the high radioactive nature of the waste.[3−10] On the other side, the literally "useless" waste could be important sources for the production of manmade nuclides which are believed to be the last missing part of the periodic table.[10−12] Although the recycling strategy for U and Pu (the majority of the nuclear waste) known as the PUREX process is well-developed, the remaining raffinate contributed mainly from minor actinides (mainly Am and Cm) is still highly radioactive in the long term, and it has a rather small elemental portion (less than 0.1%) and coexists with the chemical-similar trivalent lanthanides (Lns(III)).[3,5,6,9,13] The necessity for the separation of Lns(III) from MAs lie in two aspects: 1) the high neutron poisoning effect of some Lns(III) could reduce the transmutation efficiency of MAs into short-lived nuclides; 2) Lns showed a low tendency to form homogeneous phase in metal alloys or in mixed oxide, and they would segregate into isolated phases and grow under thermal treatments, thus leading to nonuniform heat distribution in the fuel matrix under irradiation. To effectively separate trivalent lanthanides and MAs, two approaches have been investigated, including oxidation state control and selective liquid−liquid extraction by soft donor ligands.[3,14−17] The former takes advantage of the distinct coordination geometrical differences of Am(V)/Am(VI) from Lns(III), while the latter mainly leverages the softer nature of more dispersed 5f orbitals of actinides that displayed more covalency bonding to soft donor atoms (e.g., N and S).[3,16,17] Oxidation-state-control is, in principle, more efficient than selective extraction by soft donor ligands, but the instability of the oxidized species and the inevitable introduction of corrosive reagents together with the inconsistency to the current industrial plant settings impeded the wide applications.[10,18] On the other side, selective separation by repeating the redistribution of trivalent Lns and Ans with elaborately designed soft donor ligands were featured with scalability and compatibility with multiple

Received: July 22, 2024
Revised: August 27, 2024
Accepted: August 27, 2024
Published: September 2, 2024

recovery methods for which the ligand design acts as the gamechanger.[5,6,19−22]

The search for efficient trivalent Lns and Ans separation ligands has been ongoing.[4,5,23,24] Great success has been achieved with desirable metal distribution and separation factors for target metal cations. Rooted in Hard−Soft−Acid−Base theory (HSAB), various N, S and O containing ligands were designed and utilized for Lns(III)/Ans(III) separation.[4−7,22−27] Solution species evolutions were investigated by multiple titration methods, and the coordination modes and chemical driving forces of the separation were rationalized by single crystal X-ray diffraction together with theoretical calculations.[5,9,19] Furthermore, ligand design principles such as preorganization and hard/soft-donor combined strategy for enhancing the selectivity;[9,28−32] α-effect and semirigid ligand architecture for increasing the acid resistance;[4,33] and elimination of benzyl solubilizing alkyl chains to boost the ligand radio-stability (chemical attacks under irradiation upon benzylic hydrogen has been shown to be responsible for the degradation of the ligand which could be replaced by annulated rings to boost the stability)[4,5,34] have been demonstrated and reviewed in detail. Nevertheless, ideal ligands for real-world application are still highly demanded from the prospects of high efficiency for both extraction and stripping, ease of preparation and purification, fast kinetics and superior stability.[4−6,9] Furthermore, modern recycling processes calls for a greener and more sustainable ligands' design/processing procedure to minimize the environmental impact.[7,25] As an important alternative approach, hydrophilic ligands as demonstrated in TALSPEAK and *i*-SANEX processes take advantages of unselective diglycolamides (e.g., **TODGA**) with selective back-extraction (striping) agents are promising for efficient separation of Lns(III)/Ans(III) with less hazardous organic solvent, which stands as a new frontier for *f*-block elements separations.[5,9,27,35]

Currently, the rational design principles for hydrophilic ligands are still elusive.[5,9,27] Most of the reported hydrophilic ligands were directly derived from their lipophilic counterparts through postfunctionalization with solubilizing groups such as sulfonated groups,[36−38] hydroxyl groups[39−42] and hydrophilic oligo(ethylene glycol) chains.[43] Despite the sophisticated syntheses and harsh reaction conditions, the main problem was the inferior acid resistance (referring to, particularly, the ability to extract under high acid condition), and most reported hydrophilic ligands were found to be efficient only at low acidity (smaller than 0.1 M HNO_3).[5,9,16,18,27,36−42,44−47] The reasons for the above observations could be, from our understanding, the following: 1) hydrophilic ligands were synthetically more inaccessible from both reaction control and purifications, which typically led to tedious procedure and high cost;[16,48,49] 2) the hydration enthalpies for *f*-block elements are large, which means that complexation in water should compete the strong desolvation energy, and therefore, strong coordination ligands were required to give stable complexes, which typically reduced the ligand selectivity;[50,51] 3) the high acidity of PUREX raffinates further complicated the situations as the strong competing of hydrated proton and coordinating anions could cripple the ligand from interacting with metal cations.[5,10,33] We recently proposed a series of approaches for tackling these problems. First, starting with the observation of the flipping of carbonyl group in both phenanthroline diamides and diimides from free ligands to the complexes,[18] phenanthroline diimides were recommissioned for the reduced coordination energy barrier and their potential as building blocks for the construction of highly efficient ligands for Ans(III), which have been investigated in some of the previous reports.[39,52,53] Besides, the extra hydrogen bonding on the imine sites facilitated the ligand solubilities in alcoholic solvents, which led to superior separation performances in more environmentally benign systems.[42] Further structural modifications by altering the functional ending groups flanked at both sides of phenanthroline diimides, efficient and acid tolerated Lns(III)/Ans(III) masking agents were demonstrated through crystal-engineering[16] and coordination sites protection strategies.[42] Besides, we recently illustrated that by simply altering the bonding sequences of imides with respect to the phenanthroline rings, the structural isomerides displayed totally different water solubilities, photophysics, and more importantly, the sensing abilities toward nearly identical cations of Eu(III) and Tb(III) in aqueous media.[51] Despite all this progress, the currently reported ligands still suffered from limited water solubilities (for carboxylic functionalized ligands, the ligands were only soluble in acid). To further explore the potential of phenanthroline diimides as efficient building blocks for hydrophilic ligands and to increase the ligand solubility in water to boost the ligand masking capability, new design strategies are still needed.

Herein, with the purpose of further enhancing the ligand solubility and promoting the ligand masking capability, a biomotif was introduced into the synthetic ligands for Lns(III)/Ans(III) separation. The pH sensitive protonation and deprotonation of histidine were utilized, and the motif was introduced into phenanthroline diimides framework. To facilitate ligand synthesis and purification, histidine methyl ester was introduced instead of histidine, and the group could be readily de-esterified in aqueous acid solution. The de-esterification, together with the protonation of imidazole, could increase the ligand water solubility to a large extent. The as-prepared ligand displayed superior separation ability both for Eu(III)/Am(III) and Cm(III)/Am(III) in 1.0 M HNO_3. NMR, UV−vis, and TRLFS titrations revealed the predominant formation of 1:1 coordination species during extraction. Further analysis of NMR and IR results indicated the phenanthroline diimides parts dominated the coordination in *N, O*-tetradentate manner while the histidine parts mainly contributed to the overall water solubility. We claimed that the current hydrophilic ligand design represented a novel detour to bypass sophisticated water-soluble ligand synthesis and purification. Considering the ability for both trivalent lanthanide/actinide and adjacent actinide separation abilities, the CHON compatibility, and the acid resistance (refer to the acid stability of the ligand and the stability of extraction under acid conditions), this work could be the first-of-its-kind for successful combination of biomotif and synthetic ligands for dealing with nuclear waste in a more sustainable manner.

RESULTS AND DISCUSSION

Ligand Synthesis and Characterizations

Starting from succinimide activated phenanthroline dicarboxylic acid (SI Scheme S1), synthesis of the targeting ligand of **Phen-2DIHis** was first tried by directly reacting **1** with histidine in DMSO under ambient condition. However, the successive workup of the reaction by precipitating the product from the reaction mixture failed probably due to the highly water-soluble nature of the as-formed salts (between carboxylic

https://doi.org/10.1021/jacsau.4c00659
JACS Au 2024, 4, 3668−3678

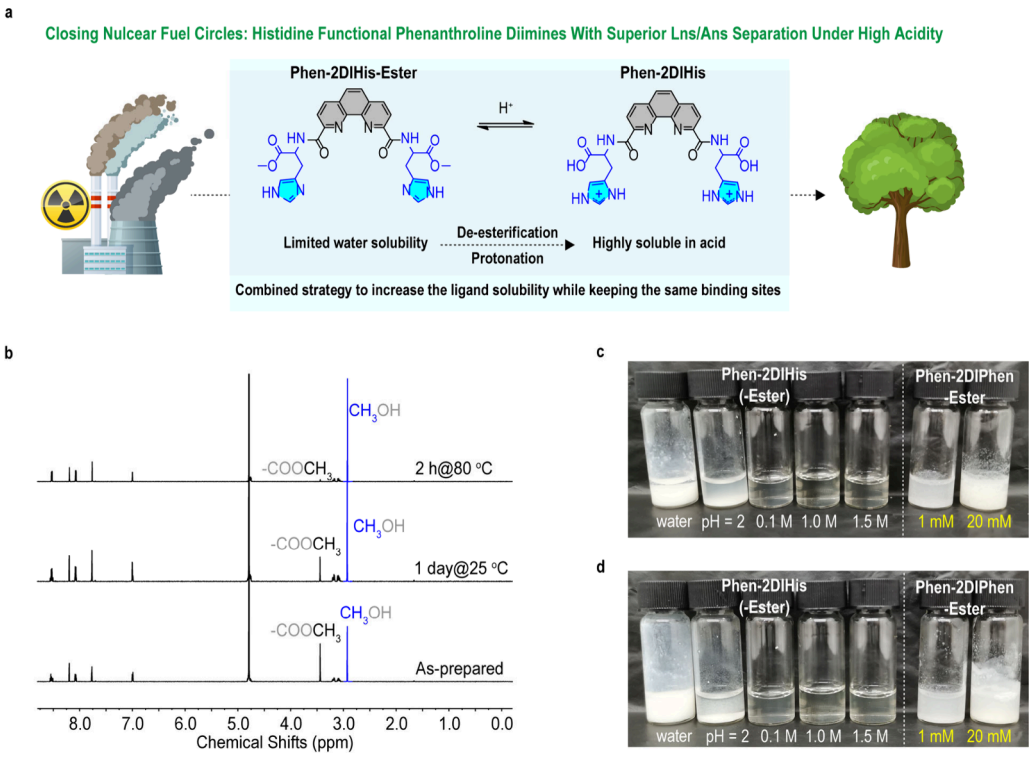

Figure 1. Identification of the ligand structure in 1.0 M HNO_3. (a) Schematic illustration of **Phen-2DIHis-Ester** and its conversion to highly soluble **Phen-2DIHis** for greener nuclear waste management. (b) NMR spectra for the as-prepared, aged (25 °C for 1 day) and heated solution (80 °C for 2 h) of 20 mM **Phen-2DIHis-Ester** in 1.0 M DNO_3/D_2O. Both de-esterification and protonation on imidazole led to the superior water solubility of the ligand as shown in panel (c, heated at 80 °C for 2 h) and (d, after cooling down to room temperature). **Phen-2DIPhen-Ester** was also investigated for confirming that the solubility enhancement was contributed from both de-esterification and protonation of histidine. Experiment conditions for (c) and (d): 20 mM **Phen-2DIHis(-Ester)** in water, pH = 2, 0.1 M, 1.0 and 1.5 M HNO_3 (left panel); 1 and 20 mM **Phen-2DIPhen-ester** in 1.0 M HNO_3 (right panel).

groups in **Phen-2DIHis** with triethylamine). Even though the product could be purified by reverse phase chromatography, this could raise the cost and purification time. Aware of the reverse nature of the esterification reaction, we bypassed the tedious synthesis and purification of **Phen-2DIHis** by preparing the ester form of **Phen-2DIHis-ester** that could be readily synthesized and purified through simple filtration. Analytically pure product could be afforded without any further purification in high yields of 80%. The ligand structure was solidly confirmed by ^1H, ^{13}C, and 2D NMR and high-resolution mass spectra (HRMS, Figure S1−4). ^1H NMR of **Phen-2DIHis-ester** in 1.0 M DNO_3/D_2O clearly revealed the existence of two different products which could be assigned to **Phen-2DIHis-ester** and **Phen-2DIHis** from the proton signals of methyl group (Figure 1b bottom trace). This assignment was further confirmed by adding external methanol, and the de-esterification could be accelerated by either prolonging the reaction time (middle trace, Figure 1b) or heating up the reaction mixture (top trace, Figure 1b). The as-formed ligand displayed excellent solubility in dilute acid with maximum concentration of over 0.1 M in 1.0 M HNO_3, which was comparable to that of sulfonated phenanthroline diimides analogues.[37,38] We claimed that the superior solubility could arise from both de-esterification and protonation of imidazole rings that typically happened at pH of around 6,[54] with more contribution from the latter. A direct comparison of phenylalanine methyl ester (**Phen-2DIPhen-ester**, Figure S5−7) under the same conditions confirmed this hypothesis for which the solubility was lower than 1 mM even after heating at 80 °C for 2 h in 1.0 M HNO_3. The in situ-formed **Phen-2DIHis** was stable in 1 M HNO_3 as reflected by the NMR spectra monitoring over 2 weeks (Figure S8). To be consistent, **Phen-2DIHis-ester** was preconditioned with 1.0 M HNO_3 at 80 °C for 2 h to fully convert to **Phen-2DIHis** before successive experiments were conducted unless otherwise stated.

Trivalent Lns(Ans)/Ans Separations

The Lns(III)/Ans(III) separation experiments were illustrated by Eu(III)/Am(III) separation. As given in Figure 2a, when **Phen-2DIHis** was used as an aqueous masking agent together with **TODGA** in dodecane as an extractant, efficient Eu(III)/Am(III) separation could be achieved with a separation factor approaching 100. The corresponding distribution ratios for Eu(III) and Am(III) were around 10 and 0.1 respectively, indicating the two metal cations could be well-separated into organic and aqueous phases, respectively. The superior separation performances of the current system were contributed mainly from the aqueous masking agent of **Phen-2DIHis** instead of **TODGA**, as under the experimental condition **TODGA** was only reported to give small $SF_{Eu(III)/Am(III)}$ of around 3.[35,42] Detailed comparison of the metal distributions indicated that the increased *SF* arose from selective masking of Am(III) with $D_{Am(III)}$ decreased by almost two magnitudes with the presence of **Phen-2DIHis** ($D_{Am(III)}$ in the range of 1−5 for **TODGA** at 1.0 M HNO_3).[35] The current reported $SF_{Eu(III)/Am(III)}$ was among the highest values under the acidity of over 1 M HNO_3.[16,36−38,40−42,44−47] Further optimization by increasing the concentrations of **TODGA** (Figure S9) or adding $NaNO_3$ (to facilitate the coordination

https://doi.org/10.1021/jacsau.4c00659
JACS Au 2024, 4, 3668−3678

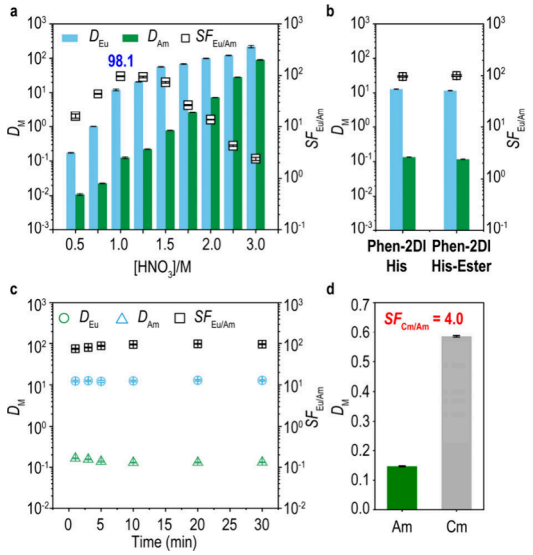

Figure 2. Demonstration of Eu(III)(Cm(III))/Am(III) separation. (a) Distribution ratios (D_M, bar graphs) and separation factors (*SF*, boxes) obtained in the extraction experiments of Eu(III) and Am(III) by **TODGA** with **Phen-2DIHis** as a function of HNO_3 concentrations. (b) Comparison of extraction performances for **Phen-2DIHis** and **Phen-2DIHis-Ester** under optimized conditions (the same as in panel a with 1.0 M HNO_3). (c) Extraction kinetics for Eu(III) and Am(III) in 1.0 M HNO_3. (d) Extraction performance for Cm(III) and Am(III) with calculated separation efficiency of 4.0 under optimized conditions from panel (a). Experiment conditions: Organic phase (O): 50 mM **TODGA** in dodecane. Aqueous phase (A): 20 mM **Phen-2DIHis-Ester** in HNO_3. O/A = 1; Vortex shaker (50 Hz) for 30 min at 25 °C. In panel (b) **Phen-2DIHis-Ester** referred to the extraction conducted immediately after dissolving **Phen-2DIHis-Ester** in 1.0 M HNO_3.

extraction, Figure S10) only increased the metal cation distributions without obviously changing the separation factors. Positive correlations between $SF_{Eu(III)/Am(III)}$ and the concentration of aqueous **Phen-2DIHis** were observed (Figure S11), because **Phen-2DIHis** helped retain metal cations in the aqueous phase (decreased $D_{Eu(III)}$ and $D_{Am(III)}$) with the preference for Am(III). It should be noted that a third phase formed during the extraction when the concentration of **Phen-2DIHis** was higher than 20 mM (Figure S12). The extent of deresterification seemed to have little impact on both metal distributions and separation factors as demonstrated in Figure 2b. Also, this indirectly indicated that the methanol generated from the decomposition of **Phen-2DIHis-Ester** had little effect on the extraction. Thus, in the current case, the introduction of histidine contributed mainly to the overall solubility of the ligand by protonation on the imidazole and de-esterification under acidic conditions. The detrimental effect on metal coordination by positively charged imidazole groups (Figure 1a) as proposed in a recent report from Mocilac in bistriazolyl-phenanthroline derivatives seemed not happen in our case[47] as revealed from both the metal cations distributions and separation factors. Furthermore, the extraction kinetics were found to be similar to other preorganized phenanthroline ligands with equilibrium reached within 5 min,[4,5,16,28,29] indicating the positive charges did not affect the coordination kinetics either under the current extraction conditions.

Besides Lns(III)/Ans(III) separation, the potential of **Phen-2DIHis** toward Ans(III)/Ans(III) separation as demonstrated in the case of Cm(III)/Am(III) was also investigated. Cm(III) and Am(III) were adjacent trivalent actinides with almost identical radii, for which the separation was believed to be more tricky:[8,55] 1) the high similarity in the chemical/physical properties of Cm(III) and Am(III) invalidated the semi-empirical prediction of their bonding characteristics differences by Person's HSAB theory, thus impeding the theoretical approaches to the design of selective ligands; 2) the highly radioactive and scarce nature of both elements hindered the efforts from trial-and-error strategy. While the practical needs for separation of Cm(III) arose from both its high neutron and heat emission that could complicate the fabrication and operation of nuclear fuel and also from its unreplaced role in the production of other strategic nuclide such as californium-252.[8,12] As shown in Figure 2d, **Phen-2DIHis** displayed obvious Am(III) selectivity with respect to Cm(III) under unoptimized conditions (the same conditions as that for Eu(III)/Am(III) extraction). The separation factor ($SF_{Cm(III)/Am(III)}$ about 4) outcompeted most of the current reported systems[8] and was superior than the benchmarked hydrophilic ligand of bis-triazolyl-pyridines[39] and bis-triazolyl-1,10-phenanthroline ligands.[40] Further optimization of the solution acidity to fine-tune the extraction abilities of **TODGA** and **Phen-2DIHis**, superior $SF_{Cm(III)/Am(III)}$ of over 4 in the acid range of 1−3 M HNO_3 with the highest value of about 7 in 1.5 M HNO_3 were observed (Figure S13), which represented the highest $SF_{Cm(III)/Am(III)}$ at this acidity (Table S1 and Scheme S2). On the other side, substituents were known to fine-tune the extraction performances especially for the adjacent *f*-elements,[56−58] we also synthesized the substituted analogues of the current ligands and the data would be present soon. It should be noted that the exact reason for the acid resistance of the reported ligand were not fully understood at this stage, while we suspected that it should be corelated to the hydrogen formation ability of imide as discussed in our recent report.[42]

To summarize, the combination of phenanthroline diimide with histidine to give **Phen-2DIHis** turned out to be an effective strategy to construct biorelevant hydrophilic trivalent actinide selective ligands. As far as we know, **Phen-2DIHis** was the first amino acid-containing ligand capable of shielding Am(III) from both Eu(III) and Cm(III) in highly acidic conditions.

Proton NMR Titrations

To have a glance on the solution coordination chemistry of **Phen-2DIHis** with *f*-block elements and shed light on the coordination species evolution for Eu(III)/Am(III) separation as discussed in the previous section, NMR titrations under the same acidity as the extraction experiments were conducted, and the results are given in Figure 3. Under the NMR titration condition of 1.0 M DNO_3/D_2O, the imidazole rings on **Phen-2DIHis** should be totally protonated, and the positive charge would be distributed on the N-C-N atoms as depicted in Figure 1a and 3 (top).[54] The NMR spectra for **Phen-2DIHis** in 1.0 M DNO_3/D_2O (Figures 3 and S14 for full spectra) was different from that in DMSO-d_6 (Figure S1) with all active protons vanished because of the fast hydrogen−deuterium exchange. The protonated **Phen-2DIHis** was highly soluble in water. The protonation reduced the electron densities on the imidazole rings and up-shifted both imidazole-associated protons (protons 7 and 8 in Figure 3, for full spectra, see Figure S14) with a much obvious chemical shift change for 8 because of its direct involvement in the positive charge

https://doi.org/10.1021/jacsau.4c00659
JACS Au 2024, 4, 3668−3678

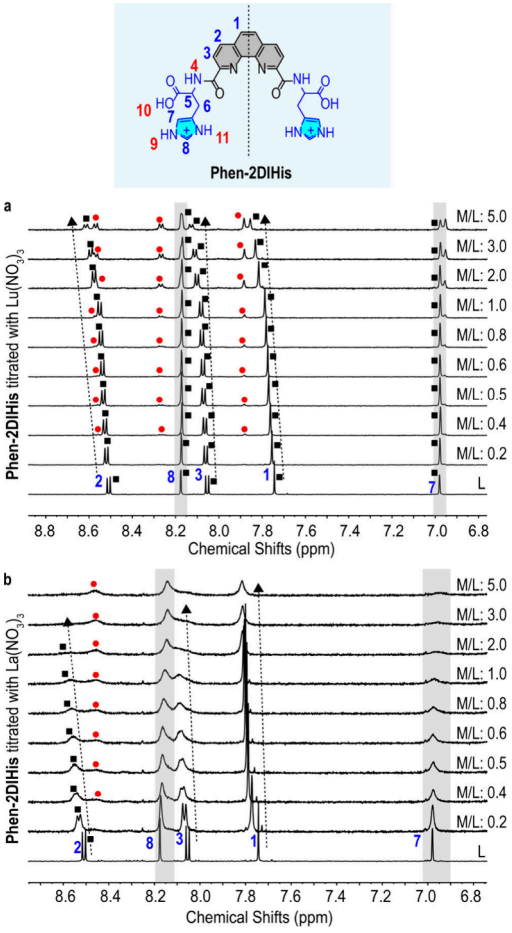

Figure 3. ^{1}H NMR titrations. Zoomed-in aromatic regions of the stacked ^{1}H NMR spectra for **Phen-2DIHis** in 1.0 M DNO_3/D_2O titrated with $Lu(NO_3)_3$ (a) and $La(NO_3)_3$ (b). The chemical structure of **Phen-2DIHis** was given on top of the figure with ligand symmetry, and half of the protons were numbered in blue (aliphatic and aromatic protons, detectable) and red (active protons). The calculated metal/ligand ratios (M/L) were given on the right side of each panel; black squares and red circles represented the evolutions for the ligand and as-formed species (M/L = 1). The dashed arrows were used for guidance. Protons' signals from imidazole rings (protons numbered 7 and 8) were marked in gray. Experiments conditions: 10 mM **Phen-2DIHis** in 1.0 M DNO_3/D_2O titrated with 0.1 M $La(NO_3)_3$ or $Lu(NO_3)_3$ at 25 °C.

delocalization. La(III) and Lu(III) cations were used for their representative ionic radii (the largest and smallest atom among the trivalent lanthanides) and their diamagnetic nature.[59] With the addition of Lu(III) into 10 mM solution of **Phen-2DIHis** in 1.0 M DNO_3/D_2O, obvious peak shifts were detected for protons originated from the phenanthroline ring (protons 1, 2 and 3 in Figure 3; full spectra in Figure S15), indicating that these protons were spatially adjacent to the coordination sites (N sits on phenanthroline ring). As expected, all protons shifted toward downfield region as the metal coordination resulted in less shielding effect on the protons. The magnitude of the shifts could reflect the coordination sites to some extent. We noticed that for the imidazole-related protons (7 and 8, the gray regions in Figure 3), the chemical shifts kept almost unchanged during the whole titrations, indicating the histidine groups might not be involved in metal coordination or, at least, not engaged for the inner sphere coordination. For M/L ratios of over 0.4, the second set of peaks appeared on the lower field side of the original signals, with the peak intensities increased with increasing M/L ratios. These two sets of peaks corresponding to the ligand and the 1:1 M/L species could still be identified at the end of titration experiment with 5 equivalents of metal cations with respect to **Phen-2DIHis**. The stability of the mixture was further evaluated, and total equilibriums were reached at the end of NMR titrations, which showed that 1) the as-formed species (1:1 M/L) were stable with an excess amount of metal cations; 2) no kinetically slow species existed under current conditions (Figure S16). When the larger metal cation La(III) was used instead of Lu(III), weaker metal−ligand interactions were detected, as reflected by the broader and weaker proton peaks (Figure 3b). The general results for Lu(III) were also valid in the case of La(III) (Figure 3b, S17 and S18). It should be pointed out that the proton peaks for the lowest-field region shifted monotonically to larger chemical shifts (lower-field region). The seemingly up-shifted broad peaks were suspected to be M/L 1 species associated with that observed for Lu(III). The NMR titration results indicated the predominant formation of 1:1 M/L species under the current liquid−liquid extraction conditions and at the same time **Phen-2DIHis** was found to be potentially capable of intragroup lanthanide discrimination. We also noticed that, the NMR titration results were distinct from that reported by Jansone-Popova on a similar but more fused phenanthroline lactam ligand, which showed narrower and uniform NMR peaks when the ligand encountered larger La(III) cations.[43]

Solution Coordination Species Analyses

Absorption titrations were versatile experimental tools for elucidate the solution coordination species evolution and thermodynamics for metal cations coordination and extraction.[5,60] Thus, UV−vis absorption titrations were conducted by gradually adding **Phen-2DIHis** into a Nd(III) solution in 1.0 M $HClO_4$ with ion strengths controlled by 1.0 M $NaClO_4$. Nd(III) was chosen for its close approximation to Am(III) in ionic radii and at the same time, and its excellent absorption property resulted from hypersensitive transitions of $^{4}I_{9/2}$ to $^{2}G_{7/2}$ and $^{4}G_{5/2}$ of Nd(III) that are sensitive to the changes of coordination environment around the metal center.[60−62] Furthermore, the spectral region of these hypersensitive transitions lay between 560 and 600 nm, far away from that of the ligand (250 to 360 nm, Figure S19), which allowed more precise analyses of the species' changes during titrations by data fitting. As given in Figure 4a, upon addition of **Phen-2DIHis** into Nd(III) solution, the superimposed transitions of $^{2}G_{7/2}$ and $^{4}G_{5/2}$ split into clear individual peaks that were previously assigned to the direct coordination of ligand toward the inner sphere of Nd(III) cations.[18,60,63] The titration was terminated when no obvious spectra changes could be detected, and the L/M of around 10 was found at the end of the titration. Fitting the titration data with nonlinear regression program *HypSpec* gave the detailed coordination species evolution and the molar absorptivity for the deconvoluted species (Figure 4b and 4c). The best-fitted results echoed well with that derived from NMR titrations indicating the predominant formation of M/L = 1 species at the end of the titration even when an excess amount of ligand/metal ratio was provided. Moreover, when metal cations such as Eu(III) were titrated into the dilute solution of **Phen-2DIHis**, the predominant 1:1 species was also identified (Figure S19).

https://doi.org/10.1021/jacsau.4c00659
JACS Au 2024, 4, 3668−3678

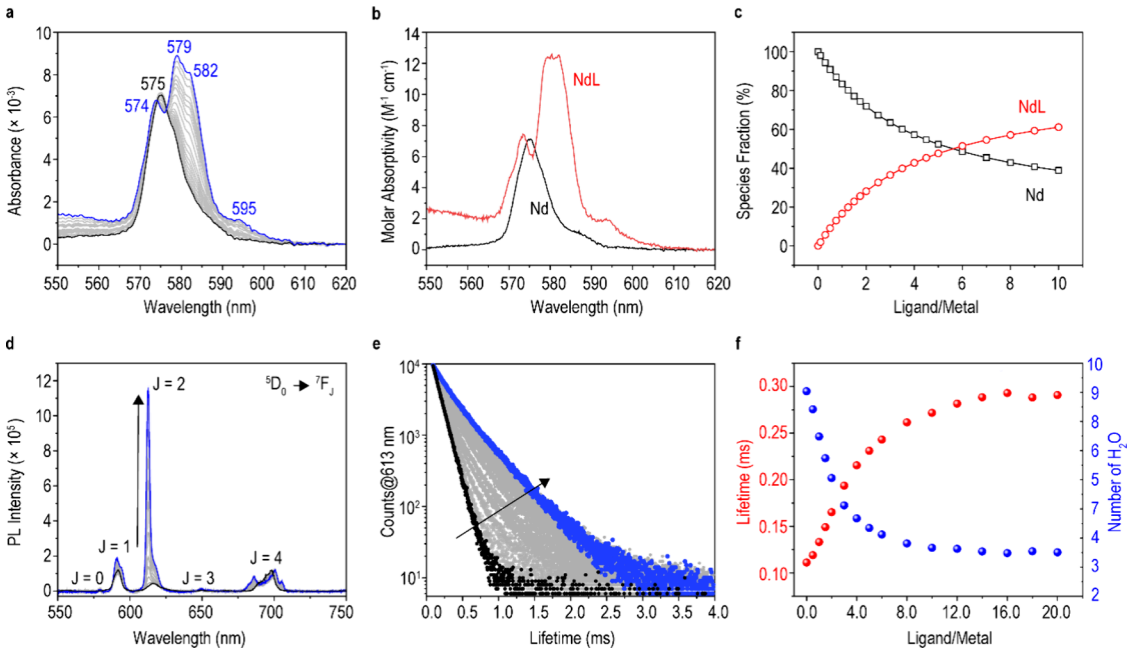

Figure 4. Demonstration of solution coordination species. (a) Absorption spectra of titration of **Phen-2DIHis** to Nd(III). Black and blue traces represented the spectra before and after the titration with main peaks marked on the figure. Experiment condition: 20 mM **Phen-2DIHis-Ester** preconditioned with 1.0 M $HClO_4$ to give **Phen-2DIHis**, ion strengths controlled by 1.0 M $NaClO_4$, 1.0 mM $Nd(ClO_4)_3$ was used for titration. Speculated species molar absorptivity (b) and species evolution (c) during titration were deduced from panel (a). TRLFS titrations of **Phen-2DIHis** to Eu(III) with characteristic Eu(III) emissions from $^5D_0$ to ^7F_J (J = 0−4). Lifetime decay curves (e) and calculated water molecules in the inner coordination sphere of Eu(III) (f) monitored at the most intense emission peak of 613 nm. Experiment condition: $C_{Ligand}/C_{Eu(III)}$ = 20 mM/1 mM in 1.0 M $HClO_4$ with 1.0 M $NaClO_4$. In total, 1.6 mL of titrant was added to V_0 = 1.6 mL of initial solution.

TRLFS titrations were another powerful tool to reveal the inner sphere coordination environment of emissive metal species.[5] In our case, **Phen-2DIHis** was titrated into Eu(III) solution in 1.0 M $HClO_4$ and the emissions from Eu(III) were monitored. As depicted in Figure 4d, well-resolved $^5D_0$ to ^7F_J (J = 0, 1, 2, 3, 4) could be detected. With the addition of **Phen-2DIHis**, water molecules were gradually excluded from the inner coordination sphere of Eu(III) by the ligand, which led to more intense emissions (Figure 4d) and prolonged lifetimes (Figure 4e).[5,64] The lifetimes at the most intense emission peak of 613 nm, corresponding to $^5D_0$ to $^7F_2$ transitions (also believed to be the most sensitive Eu(III) emission peaks associated with the coordination environment changes) were plotted as a function of ligand/metal ratios. From the lifetimes, the number of water molecules in the inner coordination sphere were deduced, and the results were given in Figure 4f (details in Supporting Information Note S1). From the TRLFS results, clear picture of the coordination could be depicted as: Eu(III) cations in 1.0 M $HClO_4$ were surrounded by 9 water molecules (ClO_4^- anions were believed to be noncoordinated) before **Phen-2DIHis** was added. The addition of the ligand excluded the water molecule around the Eu(III), giving stronger Eu(III) emission from both more effective sensitization or elimination of quenching molecules (in the current case, water). At equilibrium, ensemble-averaged 3.5 water per metal was observed, indicating the predominant of M/L = 1 species (tetradentate and positively charged **Phen-2DIHis** is expected to expel most of the water molecule in the inner coordination sphere of Eu(III)). The TRLFS results echoed those of absorption and NMR titrations. We should point out that even though Lns(III) was frequently used to surrogate An(III), they could be very different for both solution- and solid-state coordination behaviors. At last, the solution coordination behavior of radioactive Am(III) was investigated by slope analysis of the distribution ratios for Am(III) as functions of **Phen-2DIHis** concentrations under the same extraction conditions.[39,41] Linear fitting of $\log D_{Am}$ with log[**Phen-2DIHis**] gave a slope of 1.02 (Figure S20), thus indicating the predominant M/L = 1 for Am(III).

Discussions

Amino acids are by far the most important low-molecular-weight ligands in biosystems, which are involved in metal binding and recognition, enzyme catalysis/deactivation, protein folding/functionality and forming the molecular bias for multiple life-related processes.[7,65] Recent works on bioutilization of *f*-elements in biological systems further emphasized the potential application of these fundamental biomotif for the construction of ligands in *f*-elements binding and distinguishing.[22,25,66,67] Under such circumstances, two representative amino acids of histidine and phenylalanine were introduced onto phenanthroline diimides framework with the purpose to construct biohybrid hydrophilic ligands for sustainable nuclear waste management. By leveraging the reverse balance of esterification reaction and the multiple protonation properties of imidazole rings, highly water-soluble ligands of **Phen-2DIHis** were prepared in situ in rather straightforward manner, which displayed superior trivalent lanthanides/actinides and also intragroup actinides separation abilities. Competitive separation factors for Eu(III)/Am(III) of around 100 and Cm(III)/Am(III) of ca. 4 were demonstrated in 1.0 M HNO_3, which could be ranked among the best actinide masking performances under such high acidity. Some of the experimental observations in the current manuscript were further discussed as below:

https://doi.org/10.1021/jacsau.4c00659
JACS Au 2024, 4, 3668−3678

The Role of Histidine in Phen-2DIHis. As discussed in the ligand synthesis/characterization and NMR titration parts, the histidine groups helped solubilize the ligand only under acidic conditions. This could be further evidenced from the IR spectra where the carbonyl signals were unaffected during the coordination with Eu(III) (Figure S21). As IR could only be done in neutral media, methanol was used for the IR sample preparation, while the similar extraction performances for **Phen-2DIHis** and **Phen-2DIHis-Ester** as demonstrated in Figure 2b verified that the extent of de-esterification might not affect the extraction and the metal coordination, so it is reasonable for us to use IR in methanol as side evidence for metal coordination under acidic condition. Similarly, the ESI-MS results (Supporting Information Note 2, Figure S22, and Table S2) could be used to identify the coordination species. While all evidence implied the histidine groups were not involved in metal coordination, we did not deny the possibility of histidine in fine-tuning the second coordination sphere during metal coordination as recently discussed by Joseph et al. about the second-sphere interactions effect on actinides selectivity for lanmodulin.[68]

The Role of Positive Charged Terminals. Balancing water-solubility, synthetic accessibility/cost, and extraction performance were daunting tasks for effective hydrophilic ligands design. Solubilizing through ligand protonation (formation of highly soluble salts) could be the easiest way to achieve high water solubility, while the charge repulsion imposed by the positive terminals to the metal cation coordination might intuitively prevent efforts from this direction. Previous reports on some of the phenanthroline ligands also turned against this ligand design philosophy.[47] In the current report, we showed that positively charged terminals might work well for some elaborately designed systems. Even though the protonated histidine groups were thermodynamically unfavorable for metal coordination (as reflected by the absorption titrations under different conditions, see Supporting Information Note 3 and Figure S23), the kinetically strong interaction between the metal and the ligand could still guarantee the superior extraction.

Driving Force for Selective Actinides Masking. The Am(III) selectivity for the current reported ligand was investigated by DFT calculations. Both bonding nature and electron density properties for Am(III) and Eu(III) were calculated and discussed in Supporting Information Note 4. Similar to other reported phenanthroline diimides systems (both lipophilic and hydrophilic ligands),[69−72] overall shorter M−O bonds were found with respect to M−N bonds originated from the harder nature of oxygen (Figure S24, Table S3). The relative short Am(III)−N bonds compared with that of Eu(III)−N bonds indicated that the cation selectivity was mainly from N sites (also for the Cm(III)/Am(III) pair). Bader's Quantum Theory of Atoms in Molecules (QTAIM) further revealed the ionic nature for both Am(III), Eu(III) and Cm(III) in the 1:1 M/L complexes with more electron densities for both Am(III)-N and Am(III)-O at the bond critical points (BCPs) (Table S4). All of these results clearly indicated more covalency for Am(III)-based bonding than that of Eu(III) and Cm(III). Solution-state coordination experiments will be presented soon to further support the DFT results.

CONCLUSIONS

In the current work, we have reported the combination of synthetic *N, O*-polydentate ligand with amino acid to construct efficient Eu(III)/Am(III) and Cm(III)/Am(III) separation ligand under harsh acidic condition. Taking advantage of the reverse nature for esterification reaction, histidine decorated phenanthroline diimide ligands were prepared straightforwardly with high yield and purity by simple precipitation under mild reaction conditions. Furthermore, multiple protonations of histidine under acidic conditions endowed the ligand with superior solubility. Extraction performances for both Eu(III)/Am(III) and Cm(III)/Am(III) were evaluated in 1.0 M HNO_3 with **TODGA** as the lipophilic extractant. NMR, UV−vis and TRLFS titrations were conducted to reveal the solution coordination species evolutions to better understand the extraction process (for lanthanides in the current case). Together with DFT calculations, the origin of the Am(III) selectivity was discussed from both the prospects of the bonding nature and electron densities. Overall, we have proposed a simple way to construct a water-soluble and efficient trivalent lanthanide/actinide (actinide/actinide) separation ligand. At the same time, the combination of biomotif with synthetic ligands could inspire efforts in protein engineering (combination of protein with synthetic *N, O*-ligands and immobilization of protein onto solid matrix) and organic ligand modification for developing more sustainable separation ligands to relief the environmental impact (illustrated in Figure S25).

MATERIALS AND METHODS

Materials and Characterizations

All chemicals, amino acids, and ultradry solvents were purchased from Energy Chemical Inc. and used as received unless otherwise stated. Other analytically pure solvents were purchased from Bei Jing Tong Guang Fine Chemicals Company. **TODGA** was obtained from Qingdao Beitwall Technology Co., Ltd. and was used without further purification. Milli-Q water was used for all the experiments. $La(NO_3)_3{\cdot}6H_2O$ and $Lu(NO_3)_3{\cdot}6H_2O$ for NMR titrations were purchased from Aladdin with a purity of 99.99%. $Eu(ClO_4)_3$ and $Nd(ClO_4)_3$ for spectrophotometric titration experiments were prepared by dissolving Eu_2O_3 and Nd_2O_3 (Sigma-Aldrich) in perchloric acid. Stock solutions of radioactive tracers ^{244}Cm, ^{241}Am and $^{152,154}Eu$ was supplied by Institute of Nuclear and New Energy Technology (INET). *Caution:^{244}Cm,^{241}Am and$^{152,154}Eu$ are highly radioactive and radiotoxic isotopes and may pose serious health threats. And the relevant experiments were performed in a radiological facility dedicated to studies on transuranic elements.* Bis(2,5-dioxopyrrolidin-1-yl) 1,10-phenanthroline-2,9-dicarboxylate was prepared following the literature procedures.[59]

Nuclear magnetic resonance (NMR) was collected on a VARIAN-600 MHz NMR spectrometer in deuterated dimethyl sulfoxide (DMSO-d_6). High resolution mass spectrometric (HRMS) analyses were performed on a 12 T Solarix MALDI-FT-ICR MS (Bruker Daltonics). UV−vis spectra were collected on a Hitachi 3900H spectrometer with 1-cm cuvettes at 25 °C. Absorbance in the range of 250 to 600 nm (for ligand titrated with Eu(III)) and 550 to 620 nm (for Nd(III) titrations) were recorded with a scan speed of 1200 nm/min and a sampling interval of 1 nm. Fourier transform infrared (FT-IR) spectroscopy was performed on a Bruker Tensor 27 spectrometer; data were recorded in the range of 500 to 4000 cm^{-1} with a resolution of 4 cm^{-1}.

Solvent Extraction

Typical procedures for solvent extraction experiments were as follows: The aqueous phase was prepared by adding 20 mM **Phen-2DIHis** (from the hydrolysis of **Phen-2DIHis-Ester**) to nitric acid solutions

https://doi.org/10.1021/jacsau.4c00659
JACS Au 2024, 4, 3668−3678

of different acidity, and trace amount of ^{244}Cm, ^{241}Am and ^{152,154}Eu were added to the aqueous phase. Then 0.5 mL of both aqueous phase and organic phase (containing 20 mM **TODGA**, using *n*-dodecane as diluent) were contacted in a closed glass tube. To ensure fully hydrolysis of **Phen-2DIHis-Ester**, 50 mM **Phen-2DIHis-Ester** in 1.0 M HNO_3 was preconditioned by heating the solution at 80 °C for 2 h before diluting the solution to desired concentration and acidity (for higher acidity than 1.0 M HNO_3, 20 mM solutions of **Phen-2DIHis-Ester** in corresponding acid were heated under the same condition directly). The final mixtures were vigorously shaken for 30 min at a controlled temperature of 25 ± 1 °C in a water bath using a vortex shaker. After reaching equilibrium, the two phases were separated by centrifugation at 3000 rpm for 2 min. Aliquots were taken and the concentrations of ^{244}Cm, ^{241}Am and ^{152,154}Eu in both aqueous and organic phases before and after extraction were measured using a Liquid Scintillation Spectrometer (Quantulus 1220, PerkinElmer). The distribution ratio (D) was calculated as the ratio between the concentrations of radioactivity counts per volume in the organic phase and in the aqueous phase. The separation factors (SF) were determined as the ratio of distribution ratios of ^{152,154}Eu (^{244}Cm) to ^{241}Am.

Nuclear Magnetic Resonance Spectroscopy (NMR) Titrations

NMR titrations were performed on a Varian-600 spectrometer with 1.0 M DNO_3 in D_2O as the solvent. The 10 mM **Phen-2DIHis-Ester** was dissolved in 1 mL of 1.0 M DNO_3 in D_2O. The as-prepared solution was pretreated as described in the previous section then divided into two equal aliquots. 5/10 μL of stock solutions of $La(NO_3)_3$ and $Lu(NO_3)_3$ (100 mM in 1.0 M DNO_3/D_2O) were added each time, with the solution being fully mixed by inverting the NMR tubes for 5 min after each addition to equilibrate the system. The stabilities of both the ligand and the formed complexes in acidic conditions were further monitored after the NMR titration.

UV−vis Absorption Spectroscopy Titrations

UV−vis absorption titrations were conducted on a Cary 6000i UV−vis-NIR spectrophotometer (Agilent Inc.) with 1-cm cuvettes at 25 °C. In the typical reverse titration experiment where 20 mM **Phen-2DIHis** in 1.0 M $HClO_4$ were gradually added into 1.6 mL of 1.0 mM $Nd(ClO_4)_3$ in 1.0 M $HClO_4$ solution (with 1.0 M $NaClO_4$ was used to keep the ionic strength constant). The absorption of Nd(III) was monitored in the wavelength range of 550−620 nm. In the case of absorption titrations of $Eu(ClO_4)_3$, 0.4 mM $Eu(ClO_4)_3$ in 0.01 M $HClO_4$ were gradually added into 1.6 mL of 0.01 mM **Phen-2DIHis** in 0.01 M $HClO_4$ solution (with 0.1 M $NaClO_4$ to keep the ionic strength). Spectra in the range of 250−350 nm were monitored and recorded. After addition of each aliquot, the absorption spectrum was monitored after 5 min of vigorous oscillation at 25 ± 1 °C in a thermostatic oscillator to ensure complex equilibrium of the system according to our preliminary kinetic experiments. The spectral data obtained by titration were fitted with the nonlinear regression program *HypSpec* to obtain the species distributions.

Time-Resolved Laser Fluorescence Spectroscopy (TRLFS) Titrations

PL and lifetime titration of Eu(III) were recorded on an Edinburgh FLS-1000 spectrophotometer equipped with a 450 W ozone-free xenon arc lamp at 25 °C. The light source was a pulsed microsecond xenon lamp with a power of 150 W and a pulse width of ∼1 μs. In a typical titration experiment, 1.0 M $NaClO_4$ was used to keep the ionic strength constant, 20 mM **Phen-2DIHis** in 1.0 M $HClO_4$ were gradually added into 1.6 mL of 1.0 mM $Eu(ClO_4)_3$ in 1.0 M $HClO_4$ solution. Before titrations, **Phen-2DIHis-Ester** was dissolved in 1.0 M $HClO_4$ and heated in a water bath at 80 °C for 2h to ensure complete hydrolysis to **Phen-2DIHis**. The luminescence emission spectra of Eu(III) were monitored in the wavelength range of 550−720 nm (0.5 nm per step, 3 nm bandwidth) by excitation at 394 nm (electronic level of $^5L_6$, 2 nm bandwidth). After addition of each aliquot, the absorption spectrum was monitored after 5 min of vigorous oscillation at 25 ± 1 °C in a thermostatic oscillator; as in UV−vis absorption spectra titration, the operation was the same to ensure complex equilibrium. At the same time, the lifetime of the emission peak at 613 nm (corresponding to $^5D_0$ to $^7F_2$ transition of Eu(III)) were also measured. The decay data were analyzed using the software package installed on the Edinburgh FLS-1000 spectrophotometer, and the goodness of fit was assessed by minimizing the reduced function, χ^2, and visually inspecting the weighted residuals.

ESI-MS Characterizations

High-resolution mass spectrometric (HRMS) analyses were performed on a 12 T Solarix MALDI-FT-ICR MS (Bruker Daltonics). The **Phen-2DIHis-Ester**/$Eu(NO_3)_3$ mixture (ligand/metal = 1:1) was premixed and stirred in methanol at room temperature for at least 12 h before being introduced through a 15 mL stainless steel needle syringe. The nebulizer gas pressure was set to 8 psi and the operating nitrogen was 5 L/min. The source temperature was set at 200 °C and the capillary voltage was 3500 V. The ESI source in positive mode with broadband detection was used to record the data. The recorded mass typically ranged from 50 to 1200. The m/z values and absolute amplitude of all peaks were obtained using Bruker data analysis software, exported as text files.

IR Sample Preparations

Fourier transform infrared (FT-IR) spectroscopy was performed on a Bruker Tensor 27 spectrometer. Data in the range of 500 to 4000 cm^{-1} with a resolution of 4 cm^{-1} were recorded. The **Phen-2DIHis-Ester** and $Eu(NO_3)_3$ were dissolved in methanol solution according to the molar ratio of metal/ligand 1:1, and stirred at room temperature for 12 h before drying to obtain a light yellow powder solid substance. The prepared powders were mixed with KBr at a mass percentage of about 2% for further characterizations.

DFT Calculations

The geometry optimizations of **Phen-2DIHis** complexes with Eu(III), Am(III) and Cm(III) were performed by the density functional theory (DFT)[73,74] and B3LYP[75] functional using Gaussian 16. The 6-311G(d) basis set was applied for the elements in the first three periods (C, H, O, and N). The quasi-relativistic small-core pseudopotential ECP28MWB along with the corresponding ECP28MWB_SEG segment basis set were used to describe Eu(III).[76] Generally, the accuracy of the calculation results of a small nuclear pseudopotential was better than that of a large nuclear pseudopotential. And the corresponding ECP60MWB-SEG valence basis sets were used to describe Am and Cm.[77,78] Based on the results of this work, the 1:1 type configurations of $Eu(NO_3)_3$/**Phen-2DIHis**, $Am(NO_3)_3$/**Phen-2DIHis** and $Cm(NO_3)_3$/**Phen-2DIHis** were used to describe the complex structure of Eu(III), Am(III) and Cm(III). The Mayer bond order (MBO) and topological analysis were carried out by the software Mutiwfn 3.8.[79]

■ ASSOCIATED CONTENT

Supporting Information

The Supporting Information is available free of charge at https://pubs.acs.org/doi/10.1021/jacsau.4c00659.

Ligand syntheses and characterizations, ^{1}H and ^{13}C NMR spectra, 2D ^{1}H COSY NMR spectra, ESI-MS spectra, solvent extraction performances, comparison of some literature reported Cm(III)/Am(III) separation performances by liquid-based extraction, and additional supplementary data mentioned in the text (PDF)

■ AUTHOR INFORMATION

Corresponding Authors

Li Wang − *Department of Chemistry, Capital Normal University, Beijing 100048, China;* orcid.org/0000-0002-5315-0593; Email: liwang862011@gmail.com

https://doi.org/10.1021/jacsau.4c00659
JACS Au 2024, 4, 3668−3678

Chao Xu − *Institute of Nuclear and New Energy Technology, Tsinghua University, Beijing 100084, China;* orcid.org/0000-0001-5539-4754; Email: xuchao@tsinghua.edu.cn

Authors

Bin Li − *Institute of Nuclear and New Energy Technology, Tsinghua University, Beijing 100084, China; Department of Chemistry, Capital Normal University, Beijing 100048, China*

Ludi Wang − *Department of Chemistry, Capital Normal University, Beijing 100048, China; Beijing National Laboratory for Molecular Sciences, Key Laboratory of Polymer Chemistry and Physics of Ministry of Education, Centre for Soft Matter Science and Engineering, College of Chemistry and Molecular Engineering, Peking University, Beijing 100871, China*

Yu Kang − *Department of Chemistry, Capital Normal University, Beijing 100048, China*

Hong Cao − *Institute of Nuclear and New Energy Technology, Tsinghua University, Beijing 100084, China*

Yaoyang Liu − *Institute of Nuclear and New Energy Technology, Tsinghua University, Beijing 100084, China*

Qiange He − *Institute of Nuclear and New Energy Technology, Tsinghua University, Beijing 100084, China*

Zhongfeng Li − *Department of Chemistry, Capital Normal University, Beijing 100048, China*

Xiaoyan Tang − *Beijing National Laboratory for Molecular Sciences, Key Laboratory of Polymer Chemistry and Physics of Ministry of Education, Centre for Soft Matter Science and Engineering, College of Chemistry and Molecular Engineering, Peking University, Beijing 100871, China;* orcid.org/0000-0002-0050-6699

Jing Chen − *Institute of Nuclear and New Energy Technology, Tsinghua University, Beijing 100084, China*

Complete contact information is available at: https://pubs.acs.org/10.1021/jacsau.4c00659

Author Contributions

[⊥]B. Li and L.-D. Wang contributed equally to this work. B. Li, L.-D. Wang, Y. Kang, H. Cao, Y. Liu, Q. He and Z. Li: Data collection, Investigation and Validation. Y. Liu: Technical support, calculation. Z. Li: Technical support, NMR analysis. X. Tang, J. Chen, L. Wang and C. Xu: Supervision and data analysis. X. Tang, L. Wang and C. Xu: Conceptualization, Funding acquisition, Project administration. B. Li, L-D. Wang and L. Wang: Writing the original draft. L. Wang and X. Chao: review and editing. All authors have given their approval to the final version of the manuscript. CRediT: **Bin Li** data curation, investigation, validation, writing - original draft; **Ludi Wang** data curation, investigation, validation, writing - original draft; **Yu Kang** data curation, investigation, validation, writing - original draft; **Hong Cao** data curation, validation; **Yaoyang Liu** data curation, investigation, software; **Qiange He** data curation, investigation, resources, validation; **Zhongfeng Li** data curation, resources, validation; **Xiaoyan Tang** conceptualization, funding acquisition, project administration, supervision; **Jing Chen** conceptualization, project administration, supervision; **Li Wang** conceptualization, funding acquisition, project administration, supervision, writing - original draft, writing - review & editing; **Chao Xu** conceptualization, funding acquisition, project administration, supervision, validation, writing - review & editing.

Notes

The authors declare no competing financial interest.

■ ACKNOWLEDGMENTS

C.X. would like to thank National Natural Science Foundation of China (No. U2067213; 22325603); L. Wang would like to thank National Natural Science Foundation of China (22105205) and Beijing Natural Science Foundation (No. 2232002); X. Tang would like to thank the National Natural Science Foundation of China (No. 52173093) for the financial support to this work.

■ REFERENCES

(1) Fell, H.; Gilbert, A.; Jenkins, J. D.; Mildenberger, M. Nuclear power and renewable energy are both associated with national decarbonization. *Nat. Energy* **2022**, *7* (1), 25−29.

(2) Freese, L. M.; Chossière, G. P.; Eastham, S. D.; Jenn, A.; Selin, N. E. Nuclear power generation phase-outs redistribute US air quality and climate-related mortality risk. *Nat. Energy* **2023**, *8* (5), 492−503.

(3) Runde, W. H.; Mincher, B. J. Higher Oxidation States of Americium: Preparation, Characterization and Use for Separations. *Chem. Rev.* **2011**, *111* (9), 5723−5741.

(4) Hudson, M. J.; Harwood, L. M.; Laventine, D. M.; Lewis, F. W. Use of Soft Heterocyclic N-Donor Ligands To Separate Actinides and Lanthanides. *Inorg. Chem.* **2013**, *52* (7), 3414−3428.

(5) Panak, P. J.; Geist, A. Complexation and Extraction of Trivalent Actinides and Lanthanides by Triazinylpyridine N-Donor Ligands. *Chem. Rev.* **2013**, *113* (2), 1199−1236.

(6) Leoncini, A.; Huskens, J.; Verboom, W. Ligands for f-element extraction used in the nuclear fuel cycle. *Chem. Soc. Rev.* **2017**, *46* (23), 7229−7273.

(7) Götzke, L.; Schaper, G.; März, J.; Kaden, P.; Huittinen, N.; Stumpf, T.; Kammerlander, K. K. K.; Brunner, E.; Hahn, P.; Mehnert, A.; Kersting, B.; Henle, T.; Lindoy, L. F.; Zanoni, G.; Weigand, J. J. Coordination chemistry of f-block metal ions with ligands bearing bio-relevant functional groups. *Coord. Chem. Rev.* **2019**, *386*, 267−309.

(8) Matveev, P.; Mohapatra, P. K.; Kalmykov, S. N.; Petrov, V. Solvent extraction systems for mutual separation of Am(III) and Cm(III) from nitric acid solutions. A review of recent state-of-the-art. *Solvent Extr. Ion Exch.* **2021**, *39* (7), 679−713.

(9) Xu, L.; Yang, X.; Zhang, A.; Xu, C.; Xiao, C. Separation and complexation of f-block elements using hard-soft donors combined phenanthroline extractants. *Coord. Chem. Rev.* **2023**, *496*, 215404.

(10) Zsabka, P.; Wilden, A.; Van Hecke, K.; Modolo, G.; Verwerft, M.; Cardinaels, T. Beyond U/Pu separation: Separation of americium from the highly active PUREX raffinate. *J. Nucl. Mater.* **2023**, *581*, 154445.

(11) Abergel, R. J. How heavy will we get? *Nat. Chem.* **2019**, *11* (12), 1075−1075.

(12) Robinson, S. M.; Benker, D. E.; Collins, E. D.; Ezold, J. G.; Garrison, J. R.; Hogle, S. L. Production of Cf-252 and other transplutonium isotopes at Oak Ridge National Laboratory. *Radiochim. Acta* **2020**, *108* (9), 737−746.

(13) Mathur, J. N.; Murali, M. S.; Nash, K. L. ACTINIDE PARTITIONING—A REVIEW. *Solvent Extr. Ion Exch.* **2001**, *19* (3), 357−390.

(14) Dares, C. J.; Lapides, A. M.; Mincher, B. J.; Meyer, T. J. Electrochemical oxidation of ^{243}Am(III) in nitric acid by a terpyridyl-derivatized electrode. *Science* **2015**, *350* (6261), 652−655.

(15) Wang, Z.; Lu, J.-B.; Dong, X.; Yan, Q.; Feng, X.; Hu, H.-S.; Wang, S.; Chen, J.; Li, J.; Xu, C. Ultra-Efficient Americium/Lanthanide Separation through Oxidation State Control. *J. Am. Chem. Soc.* **2022**, *144* (14), 6383−6389.

(16) Tian, D.; Liu, Y.; Kang, Y.; Zhao, Y.; Li, P.; Xu, C.; Wang, L. A Simple yet Efficient Hydrophilic Phenanthroline-Based Ligand for Selective Am(III) Separation under High Acidity. *ACS Cent. Sci.* **2023**, *9* (8), 1642−1649.

(17) Zhang, H.; Li, A.; Li, K.; Wang, Z.; Xu, X.; Wang, Y.; Sheridan, M. V.; Hu, H.-S.; Xu, C.; Alekseev, E. V.; Zhang, Z.; Yan, P.; Cao, K.; Chai, Z.; Albrecht-Schönzart, T. E.; Wang, S. Ultrafiltration separation of Am(VI)-polyoxometalate from lanthanides. *Nature* **2023**, *616* (7957), 482−487.
(18) Liu, Y.; Bao, M.; Wang, L.; Kang, Y.; Dou, Y.; Qin, J.; Guo, F.; Hao, H.; Wang, Z.; Tang, X.; Chen, J.; Wang, L.; Xu, C. Ligand structure optimization leads to efficient acid-resist Am(III)/Eu(III) separation in n-octanol. *Chem. Eng. J.* **2024**, *485*, 149730.
(19) Lan, J.-H.; Shi, W.-Q.; Yuan, L.-Y.; Li, J.; Zhao, Y.-L.; Chai, Z.-F. Recent advances in computational modeling and simulations on the An(III)/Ln(III) separation process. *Coord. Chem. Rev.* **2012**, *256* (13), 1406−1417.
(20) Wilson, A. M.; Bailey, P. J.; Tasker, P. A.; Turkington, J. R.; Grant, R. A.; Love, J. B. Solvent extraction: the coordination chemistry behind extractive metallurgy. *Chem. Soc. Rev.* **2014**, *43* (1), 123−134.
(21) Florek, J.; Giret, S.; Juère, E.; Larivière, D.; Kleitz, F. Functionalization of mesoporous materials for lanthanide and actinide extraction. *Dalton Trans.* **2016**, *45* (38), 14832−14854.
(22) Cheisson, T.; Schelter, E. J. Rare earth elements: Mendeleev's bane, modern marvels. *Science* **2019**, *363* (6426), 489−493.
(23) Dam, H. H.; Reinhoudt, D. N.; Verboom, W. Multicoordinate ligands for actinide/lanthanide separations. *Chem. Soc. Rev.* **2007**, *36* (2), 367−377.
(24) Yang, X.; Xu, L.; Zhang, A.; Xiao, C. Organophosphorus Extractants: A Critical Choice for Actinides/Lanthanides Separation in Nuclear Fuel Cycle. *Chem. - Eur. J.* **2023**, *29* (33), No. e202300456.
(25) Mattocks, J. A.; Cotruvo, J. A. Biological, biomolecular, and bio-inspired strategies for detection, extraction, and separations of lanthanides and actinides. *Chem. Soc. Rev.* **2020**, *49* (22), 8315−8334.
(26) Archer, E. M.; Galley, S. S.; Jackson, J. A.; Shafer, J. C. Investigation of f-Element Interactions with Functionalized Diamides of Phenanthroline-Based Ligands. *Solvent Extr. Ion Exch.* **2023**, *41* (6), 697−740.
(27) Wang, Y.; Shield, K. M.; Abergel, R. J. Hydrophilic Chelators for Aqueous Reprocessing of Spent Nuclear Fuel. *Sep. Purif. Rev.* **2024**, *53*, 119−137.
(28) Lewis, F. W.; Harwood, L. M.; Hudson, M. J.; Drew, M. G. B.; Desreux, J. F.; Vidick, G.; Bouslimani, N.; Modolo, G.; Wilden, A.; Sypula, M.; Vu, T.-H.; Simonin, J.-P. Highly Efficient Separation of Actinides from Lanthanides by a Phenanthroline-Derived Bis-triazine Ligand. *J. Am. Chem. Soc.* **2011**, *133* (33), 13093−13102.
(29) Lewis, F. W.; Harwood, L. M.; Hudson, M. J.; Drew, M. G. B.; Hubscher-Bruder, V.; Videva, V.; Arnaud-Neu, F.; Stamberg, K.; Vyas, S. BTBPs versus BTPhens: Some Reasons for Their Differences in Properties Concerning the Partitioning of Minor Actinides and the Advantages of BTPhens. *Inorg. Chem.* **2013**, *52* (9), 4993−5005.
(30) Xiao, C.-L.; Wang, C.-Z.; Yuan, L.-Y.; Li, B.; He, H.; Wang, S.; Zhao, Y.-L.; Chai, Z.-F.; Shi, W.-Q. Excellent Selectivity for Actinides with a Tetradentate 2,9-Diamide-1,10-Phenanthroline Ligand in Highly Acidic Solution: A Hard-Soft Donor Combined Strategy. *Inorg. Chem.* **2014**, *53* (3), 1712−1720.
(31) Jansone-Popova, S.; Ivanov, A. S.; Bryantsev, V. S.; Sloop, F. V., Jr; Custelcean, R.; Popovs, I.; Dekarske, M. M.; Moyer, B. A. Bis-lactam-1,10-phenanthroline (BLPhen), a New Type of Preorganized Mixed N,O-Donor Ligand That Separates Am(III) over Eu(III) with Exceptionally High Efficiency. *Inorg. Chem.* **2017**, *56* (10), 5911−5917.
(32) Healy, M. R.; Ivanov, A. S.; Karslyan, Y.; Bryantsev, V. S.; Moyer, B. A.; Jansone-Popova, S. Efficient Separation of Light Lanthanides(III) by Using Bis-Lactam Phenanthroline Ligands. *Chem. - Eur. J.* **2019**, *25* (25), 6326−6331.
(33) Wang, S.; Wang, C.; Yang, X.-f.; Yu, J.-p.; Tao, W.-q.; Yang, S.-l.; Ren, P.; Yuan, L.-y.; Chai, Z.-f.; Shi, W.-q. Selective Separation of Am(III)/Eu(III) by the QL-DAPhen Ligand under High Acidity: Extraction, Spectroscopy, and Theoretical Calculations. *Inorg. Chem.* **2021**, *60* (24), 19110−19119.
(34) Fermvik, A.; Berthon, L.; Ekberg, C.; Englund, S.; Retegan, T.; Zorz, N. Radiolysis of solvents containing C5-BTBP: identification of degradation products and their dependence on absorbed dose and dose rate. *Dalton Trans.* **2009**, No. 32, 6421−6430.
(35) Ansari, S. A.; Pathak, P. N.; Manchanda, V. K.; Husain, M.; Prasad, A. K.; Parmar, V. S. N,N,N′,N′-Tetraoctyl Diglycolamide (TODGA): A Promising Extractant for Actinide-Partitioning from High-Level Waste (HLW). *Solvent Extr. Ion Exch.* **2005**, *23* (4), 463−479.
(36) Geist, A.; Müllich, U.; Magnusson, D.; Kaden, P.; Modolo, G.; Wilden, A.; Zevaco, T. Actinide(III)/Lanthanide(III) Separation Via Selective Aqueous Complexation of Actinides(III) using a Hydrophilic 2,6-Bis(1,2,4-Triazin-3-Yl)-Pyridine in Nitric Acid. *Solvent Extr. Ion Exch.* **2012**, *30* (5), 433−444.
(37) Lewis, F. W.; Harwood, L. M.; Hudson, M. J.; Geist, A.; Kozhevnikov, V. N.; Distler, P.; John, J. Hydrophilic sulfonated bis-1,2,4-triazine ligands are highly effective reagents for separating actinides(iii) from lanthanides(iii) via selective formation of aqueous actinide complexes. *Chem. Sci.* **2015**, *6* (8), 4812−4821.
(38) Ren, P.; Huang, P.-w.; Yang, X.-f.; Zou, Y.; Tao, W.-q.; Yang, S.-l.; Liu, Y.-h.; Wu, Q.-y.; Yuan, L.-y.; Chai, Z.-f.; Shi, W.-q. Hydrophilic Sulfonated 2,9-Diamide-1,10-phenanthroline Endowed with a Highly Effective Ligand for Separation of Americium(III) from Europium-(III): Extraction, Spectroscopy, and Density Functional Theory Calculations. *Inorg. Chem.* **2021**, *60* (1), 357−365.
(39) Macerata, E.; Mossini, E.; Scaravaggi, S.; Mariani, M.; Mele, A.; Panzeri, W.; Boubals, N.; Berthon, L.; Charbonnel, M.-C.; Sansone, F.; Arduini, A.; Casnati, A. Hydrophilic Clicked 2,6-Bis-triazolyl-pyridines Endowed with High Actinide Selectivity and Radiochemical Stability: Toward a Closed Nuclear Fuel Cycle. *J. Am. Chem. Soc.* **2016**, *138* (23), 7232−7235.
(40) Edwards, A. C.; Mocilac, P.; Geist, A.; Harwood, L. M.; Sharrad, C. A.; Burton, N. A.; Whitehead, R. C.; Denecke, M. A. Hydrophilic 2,9-bis-triazolyl-1,10-phenanthroline ligands enable selective Am(iii) separation: a step further towards sustainable nuclear energy. *Chem. Commun.* **2017**, *53* (36), 5001−5004.
(41) Weßling, P.; Maag, M.; Baruth, G.; Sittel, T.; Sauerwein, F. S.; Wilden, A.; Modolo, G.; Geist, A.; Panak, P. J. Complexation and Extraction Studies of Trivalent Actinides and Lanthanides with Water-Soluble and CHON-Compatible Ligands for the Selective Extraction of Americium. *Inorg. Chem.* **2022**, *61* (44), 17719−17729.
(42) Liu, Y.; Kang, Y.; Bao, M.; Cao, H.; Weng, C.; Dong, X.; Hao, H.; Tang, X.; Chen, J.; Wang, L.; Xu, C. Hydroxyl-group functionalized phenanthroline diimides as efficient masking agents for Am(III)/Eu(III) separation under harsh conditions. *J. Hazard. Mater.* **2024**, *462*, 132756.
(43) Johnson, K. R.; Driscoll, D. M.; Damron, J. T.; Ivanov, A. S.; Jansone-Popova, S. Size Selective Ligand Tug of War Strategy to Separate Rare Earth Elements. *JACS Au.* **2023**, *3* (2), 584−591.
(44) Bhattacharyya, A.; Gadly, T.; Kanekar, A. S.; Ghosh, S. K.; Kumar, M.; Mohapatra, P. K. First Report on the Separation of Trivalent Lanthanides from Trivalent Actinides Using an Aqueous Soluble Multiple N-Donor Ligand, 2,6-bis(1H-tetrazol-5-yl)pyridine: Extraction, Spectroscopic, Structural, and Computational Studies. *Inorg. Chem.* **2018**, *57* (9), 5096−5107.
(45) Wu, Q.; Hao, H.; Liu, Y.; Sha, L.-T.; Wang, W.-J.; Shi, W.-q.; Wang, Z.; Yan, Z.-Y. Selective Separation of Americium(III), Curium(III), and Lanthanide(III) by Aqueous and Organic Competitive Extraction. *Inorg. Chem.* **2024**, *63* (1), 462−473.
(46) He, L.; Wang, X.; Li, Q.; Xiao, X.; Li, F.; Luo, F.; Pan, Q.; Ding, S. Novel water-soluble aromatic bisdiglycolamide masking agents for the separation of trivalent americium over lanthanides by NTAamide-(n-Oct) extractant. *J. Environ. Chem. Eng.* **2023**, *11* (2), 109536.
(47) Wan, Y. Q.; Hao, H.; Yu, L.; Wang, Z. P.; Mocilac, P. Novel hydrophilic bistriazolyl-phenanthroline ligands with improved solubility and performance in An/Ln separations. *RSC Adv.* **2023**, *13* (32), 21982−21990.
(48) Chatterton, N.; Bretonnière, Y.; Pécaut, J.; Mazzanti, M. An Efficient Design for the Rigid Assembly of Four Bidentate

https://doi.org/10.1021/jacsau.4c00659
JACS Au 2024, 4, 3668−3678

Chromophores in Water-Stable Highly Luminescent Lanthanide Complexes. *Angew. Chem., Int. Ed.* **2005**, *44* (46), 7595−7598.
(49) Moore, E. G.; Xu, J.; Jocher, C. J.; Werner, E. J.; Raymond, K. N. "Cymothoe sangaris": An Extremely Stable and Highly Luminescent 1,2-Hydroxypyridinonate Chelate of Eu(III). *J. Am. Chem. Soc.* **2006**, *128* (33), 10648−10649.
(50) Bünzli, J.-C. G. Review: Lanthanide coordination chemistry: from old concepts to coordination polymers. *J. Coord. Chem.* **2014**, *67* (23−24), 3706−3733.
(51) Kang, Y.; Li, H.; Bao, M.; Zheng, Y.; Wang, L.; Liu, D.; Li, J.; Wei, Z.; Weng, C.; Wang, G.; Tang, X.; Wang, L. A step forward in unraveling the lanthanide discrimination puzzle: structure-selectivity relationship based on phenanthroline diimide ligands towards europium and terbium detection in water. *J. Mater. Chem. C* **2024**, *12* (17), 6056−6063.
(52) Scaravaggi, S.; Macerata, E.; Galletta, M.; Mossini, E.; Casnati, A.; Anselmi, M.; Sansone, F.; Mariani, M. Hydrophilic 1,10-phenanthroline derivatives for selective Am(III) stripping into aqueous solutions. *J. Radioanal. Nucl. Chem.* **2014**, *303* (3), 1811−1820.
(53) Manna, D.; Mula, S.; Bhattacharyya, A.; Chattopadhyay, S.; Ghanty, T. K. Actinide selectivity of 1,10-phenanthroline-2,9-dicarboxamide and its derivatives: a theoretical prediction followed by experimental validation. *Dalton Trans.* **2015**, *44* (3), 1332−1340.
(54) Li, S.; Hong, M. Protonation, Tautomerization, and Rotameric Structure of Histidine: A Comprehensive Study by Magic-Angle-Spinning Solid-State NMR. *J. Am. Chem. Soc.* **2011**, *133* (5), 1534−1544.
(55) Lewis, F. W.; Harwood, L. M.; Hudson, M. J.; Afsar, A.; Laventine, D. M.; Šťastná, K.; John, J.; Distler, P. Separation of the Minor Actinides Americium(III) and Curium(III) by Hydrophobic and Hydrophilic BTPhen ligands: Exploiting Differences in their Rates of Extraction and Effective Separations at Equilibrium. *Solvent Extr. Ion Exch.* **2018**, *36* (2), 115−135.
(56) Afsar, A.; Laventine, D. M.; Harwood, L. M.; Hudson, M. J.; Geist, A. Utilizing electronic effects in the modulation of BTPhen ligands with respect to the partitioning of minor actinides from lanthanides. *Chem. Commun.* **2013**, *49* (76), 8534−8536.
(57) Ustynyuk, Y. A.; Borisova, N. E.; Babain, V. A.; Gloriozov, I. P.; Manuilov, A. Y.; Kalmykov, S. N.; Alyapyshev, M. Y.; Tkachenko, L. I.; Kenf, E. V.; Ustynyuk, N. A. N,N′-Dialkyl-N,N′-diaryl-1,10-phenanthroline-2,9-dicarboxamides as donor ligands for separation of rare earth elements with a high and unusual selectivity. DFT computational and experimental studies. *Chem. Commun.* **2015**, *51* (35), 7466−7469.
(58) Evsiunina, M. V.; Khult, E. K.; Matveev, P. I.; Kalle, P.; Lemport, P. S.; Petrov, V. S.; Aksenova, S. A.; Nelyubina, Y. V.; Koshelev, D. S.; Utochnikova, V. V.; Petrov, V. G.; Ustynyuk, Y. A.; Nenajdenko, V. G. Unravelling the mechanism of f-element extraction by phenanthroline-diamides: A case of 4,7-substituted 1,10-phenanthroline-2,9-diamides. *Sep. Purif. Technol.* **2024**, *339*, 126621.
(59) Duan, L.; Fan, J.; Tian, D.; Yan, Q.; Zhang, X.; Li, P.; Xu, C.; Wang, L. A novel and versatile precursor for the synthesis of highly preorganized tetradentate ligands based on phenanthroline and their binding properties towards lanthanides(III) ions. *Colloid Surf. A-Physicochem. Eng. Asp.* **2022**, *647*, 129089.
(60) Nawrocki, P. R.; Sørensen, T. J. Optical spectroscopy as a tool for studying the solution chemistry of neodymium(iii). *Phys. Chem. Chem. Phys.* **2023**, *25* (29), 19300−19336.
(61) Henrie, D. E.; Choppin, G. R. Environmental Effects on f-f Transitions. II. "Hypersensitivity" in Some Complexes of Trivalent Neodymium. *J. Chem. Phys.* **1968**, *49* (2), 477−481.
(62) Kumar, S.; Maji, S.; Sundararajan, K. Nd(III) hypersensitive peak as an optical absorption probe for determining nitric acid in aqueous solution: An application to aqueous raffinate solutions in nuclear reprocessing. *Talanta* **2021**, *231*, 122398.
(63) Tian, G.; Teat, S. J.; Rao, L. Structural and Thermodynamic Study of the Complexes of Nd(III) with N,N,N′,N′-Tetramethyl-3-oxa-glutaramide and the Acid Analogues. *Inorg. Chem.* **2014**, *53* (18), 9477−9485.
(64) Horrocks, W. D., Jr; Sudnick, D. R. Lanthanide ion probes of structure in biology. Laser-induced luminescence decay constants provide a direct measure of the number of metal-coordinated water molecules. *J. Am. Chem. Soc.* **1979**, *101* (2), 334−340.
(65) Kremer, C.; Torres, J.; Domínguez, S.; Mederos, A. Structure and thermodynamic stability of lanthanide complexes with amino acids and peptides. *Coord. Chem. Rev.* **2005**, *249* (5), 567−590.
(66) Cotruvo, J. A., Jr The Chemistry of Lanthanides in Biology: Recent Discoveries, Emerging Principles, and Technological Applications. *ACS Cent. Sci.* **2019**, *5* (9), 1496−1506.
(67) Mattocks, J. A.; Jung, J. J.; Lin, C.-Y.; Dong, Z.; Yennawar, N. H.; Featherston, E. R.; Kang-Yun, C. S.; Hamilton, T. A.; Park, D. M.; Boal, A. K.; Cotruvo, J. A. Enhanced rare-earth separation with a metal-sensitive lanmodulin dimer. *Nature* **2023**, *618* (7963), 87−93.
(68) Mattocks, J. A.; Cotruvo, J. A.; Deblonde, G. J. P. Engineering lanmodulin's selectivity for actinides over lanthanides by controlling solvent coordination and second-sphere interactions. *Chem. Sci.* **2022**, *13* (20), 6054−6066.
(69) Huang, P.-W. Theoretical unraveling of the separation of trivalent Am and Eu ions by phosphine oxide ligands with different central heterocyclic moieties. *Dalton Trans.* **2022**, *51* (18), 7118−7126.
(70) Wang, C.; Wu, Q.-Y.; Wang, C.-Z.; Lan, J.-H.; Nie, C.-M.; Chai, Z.-F.; Shi, W.-Q. Theoretical insights into selective separation of trivalent actinide and lanthanide by ester and amide ligands based on phenanthroline skeleton. *Dalton Trans.* **2020**, *49* (13), 4093−4099.
(71) Zou, Y.; Lan, J.-H.; Yuan, L.-Y.; Wang, C.-Z.; Wu, Q.-Y.; Chai, Z.-F.; Ren, P.; Shi, W.-Q. Theoretical Insights into the Selectivity of Hydrophilic Sulfonated and Phosphorylated Ligands to Am(III) and Eu(III) Ions. *Inorg. Chem.* **2023**, *62* (11), 4581−4589.
(72) Huang, P.-W.; Wang, C.-Z.; Wu, Q.-Y.; Lan, J.-H.; Chai, Z.-F.; Shi, W.-Q. Enhanced Am/Eu separation ability of disulfonated diamide N-heterocyclic ligands by adjusting N-, O-donor affinity: A theoretical comparative study. *Sep. Purif. Technol.* **2023**, *319*, 124030.
(73) Hohenberg, P.; Kohn, W. Inhomogeneous Electron Gas. *Phys. Rev.* **1964**, *136* (3B), B864−B871.
(74) Kohn, W.; Sham, L. J. Self-Consistent Equations Including Exchange and Correlation Effects. *Phys. Rev.* **1965**, *140* (4A), A1133−A1138.
(75) Lee, C.; Yang, W.; Parr, R. G. Development of the Colle-Salvetti correlation-energy formula into a functional of the electron density. *Phys. Rev. B* **1988**, *37* (2), 785−789.
(76) Cao, X.; Dolg, M. Segmented contraction scheme for small-core lanthanide pseudopotential basis sets. *J. Mol. Struc-THEOCHM.* **2002**, *581* (1), 139−147.
(77) Cao, X. New Basis Sets for Lanthanide and Actinide Energy-consistent Small-core Pseudopotentials. *J. Chin. Chem. Soc.* **2003**, *50* (3B), 665−676.
(78) Cao, X.; Dolg, M. Segmented contraction scheme for small-core actinide pseudopotential basis sets. *J. Mol. Struc-THEOCHM.* **2004**, *673* (1), 203−209.
(79) Lu, T.; Chen, F. Multiwfn: A multifunctional wavefunction analyzer. *J. Comput. Chem.* **2012**, *33* (5), 580−592.

https://doi.org/10.1021/jacsau.4c00659
JACS Au 2024, 4, 3668−3678